VII Jornades IdISBa

PÒSTERS DE L'ÀREA:

Malalties Infeccioses, Resistència Antibiòtica i Resposta Immunològica

Institut d'Investigació Sanitària Illes Balears

IdISBa

A Wearable Analytical Platform with Enzyme-Modulated Dynamic Range for Simultaneous Colorimectric Detection of Sweat Volume and Sweat Biomarkers.

Andreu Vaquer[a], Enrique Barón[a], Roberto de la Rica[a]

[a]Multidisciplinary Sepsis Group, Health Research Institute of the Balearic Islands (IdISBa), Son Espases University Hospital, 07120 Palma de Mallorca, Spain.

Introduction

Colorimetric biosensors are becoming increasingly popular because the test result can be directly read with a mobile device. This is key in the case of wearable biosensors, which are directly attached to the patient's skin and the colorimetric signal can be read with the patient's smartphone. For quantitative measures, the sample volume must be controlled. To reach this goal, we developed an analytical platform that simultaneously measures lactate concentration in sweat and the sweat volume. Using this device we were able to measure lactate levels during an exercise routine in a group of volunteers, independently of the wearer's sweat rate.

Experimental section

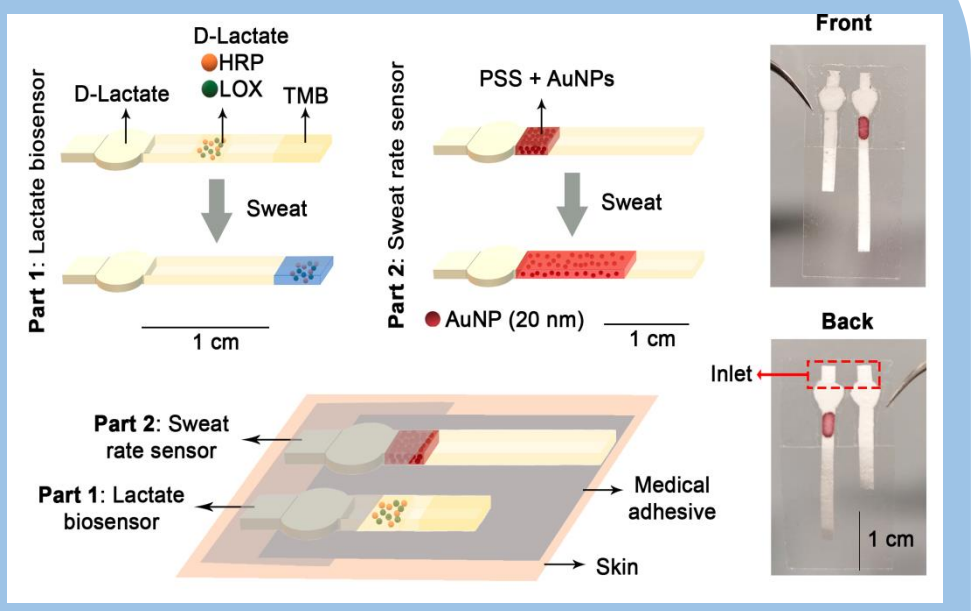

The peroxidase-mediated oxidation of TMB using the H_2O_2 generated by LOX was used to detect L- Lactate. By adding a competitive inhibitor of LOX (D-Lactate) the dynamic range of the lactate biosensor can be fine-tuned. The sweat volume sensor contains a AuNPs reservoir. As the wearer sweats, the nanoparticles are carried through the paper strip and the sweat volume can be measured calorimetrically.

Conclusions

A colorimetric analytical platform capable of measuring lactate in sweat and correct the colorimetric signal for the sweat volume was developed. Furthermore, the biosensor was applied and validated in a real case scenario with healthy volunteers. In the future, the biosensor can be combined with healthcare applications and even adapted to detect other biomarkers by changing the used oxidoreductase.

Results

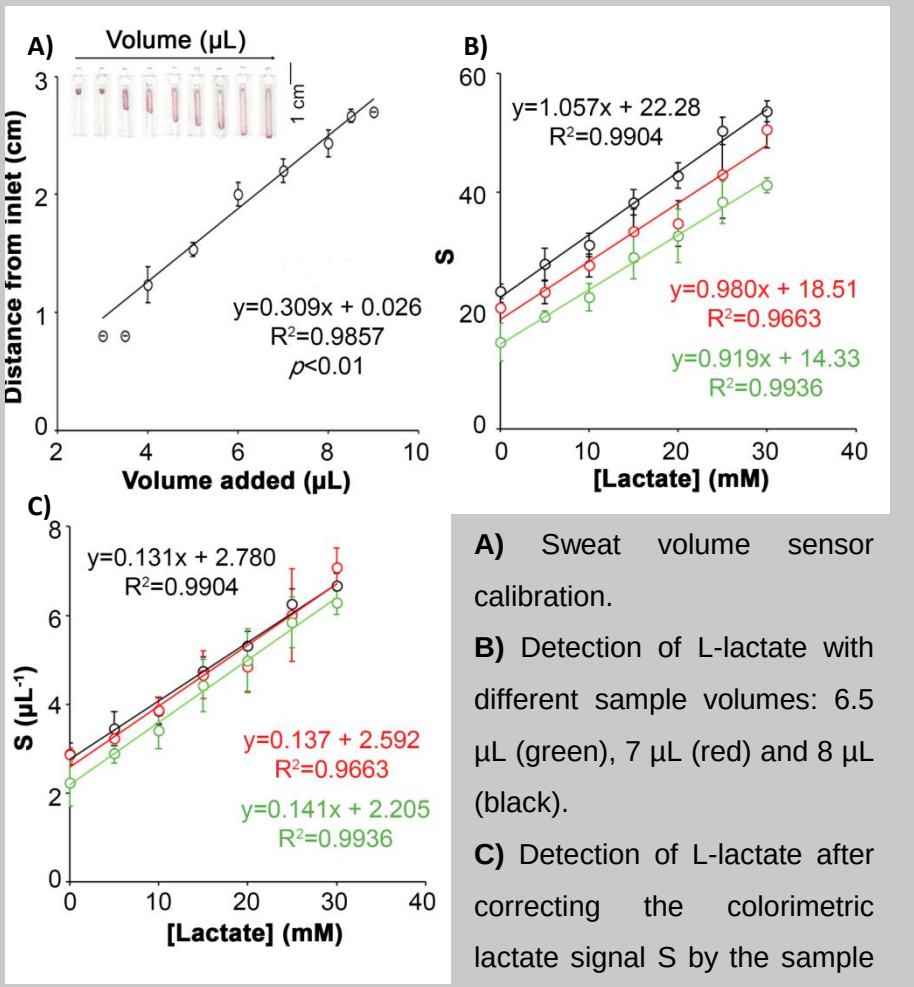

A) Sweat volume sensor calibration.

B) Detection of L-lactate with different sample volumes: 6.5 µL (green), 7 µL (red) and 8 µL (black).

C) Detection of L-lactate after correcting the colorimetric lactate signal S by the sample volume measured with the sweat volume sensor (µL).

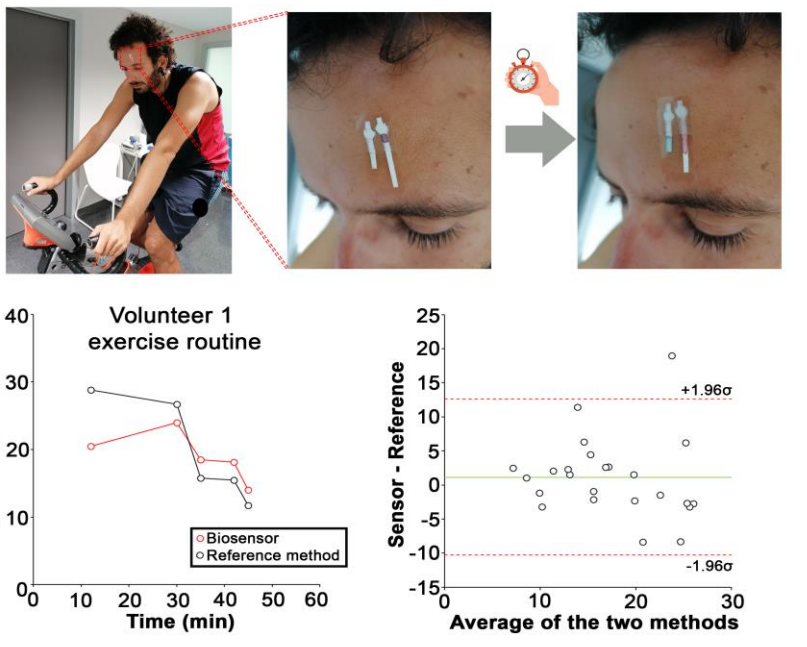

The analitical platform was used to measure lactate in 5 volunteers. Bland-Altman plot representing all measures (n=25) shows that both methods are equivalent.

- Nanoparticle Reservoirs for Paper-Only Immunosensors
Alejandra Alba-Patiño, Cristina Adrover-Jaume, and Roberto de la Rica
ACS Sensors 2020 5 (1), 147-153
DOI: 10.1021/acssensors.9b01937

- Patent: "process of storing and releasing protein-decorated nanoparticles on paper substrates" nº: 201930784

Paper Biosensors for Detecting Elevated Cytokine Levels in Blood and Respiratory Samples from COVID-19 Patients

Cristina Adrover-Jaume[a], Alejandra Alba-Patiño[a], Antonio Clemente[a], Giulia Santopolo[a], Andreu Vaquer[a], Steven M. Russell[a], Enrique Barón[a], María del Mar González del Campo[a], Juana M. Ferrer[b], María Berman-Riu[b], Mercedes García-Gasalla[c], María Aranda[a], Marcio Borgesa and Roberto de la Rica[a].

[a] Multidisciplinary Sepsis Group, IdISBa / [b]Immune Response in Human Pathology Group, IdISBa / [c]Infectious Diseases-HIV Group, IdISBa

INTRODUCTION

RAPID
Results in 10 minutes

BETTER SENSITIVITY
with nanomaterials

PAPER-ONLY IMMUNOSENSOR
Inexpensive and biodegradable

LOW LIMIT OF DETECTION
10^{-3} pg mL^{-1}

POINT OF CARE DETECTION
with a phone app

The SARS-CoV-2 pandemic has rapidly spread worldwide with enormous social and economic repercussions.[1] During the pandemic peak, saturation of hospitals forced healthcare providers to decentralize COVID-19 care.[2] For this reason, there is an urgent need for home testing biomarkers that indicate progression to severe COVID-19.[3]

In order to cover this need, we have designed a rapid test for detecting prognostic biomarkers of COVID-19 in blood and respiratory samples. Specifically, these immunosensors were utilized for detecting IL-6.

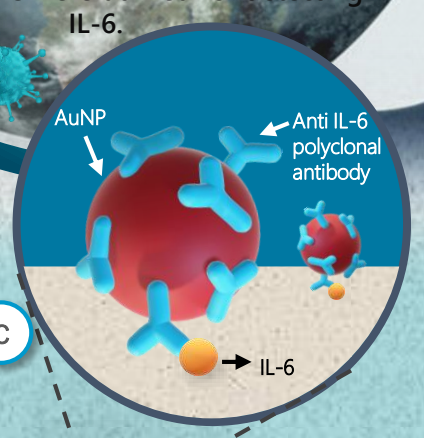

EXPERIMENTAL METHOD

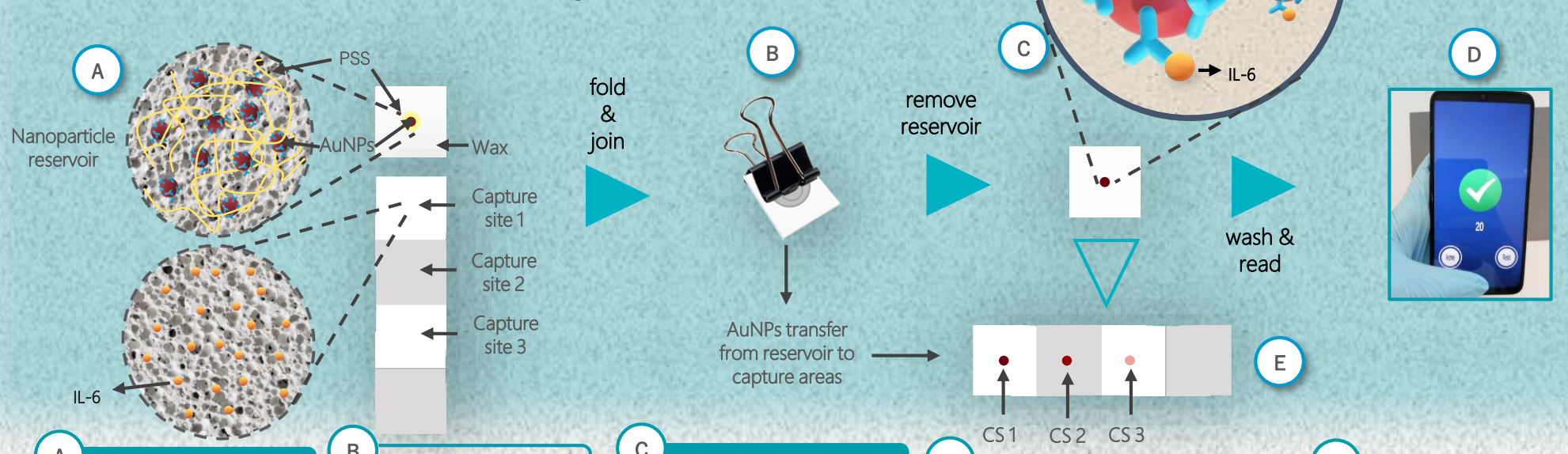

A The biosensors consist of a piece of paper containing antibody-decorated nanoparticles, and a paper strip with three capture sites (CS).

B After adding a drop of sample in each capture site and drying it, the paper is folded, and the reservoir is pressed onto CS1 for 5 min.

C After removing the reservoir, a colored spot appears whose pixel intensity is the sum of the colorimetric signal generated in each capture site.

D After washing away excess reagents the colorimetric signal is measured with a previously developed smartphone app within seconds.

E Unfolding the paper strip in (C) reveals that nanoparticles are transferred vertically to the 3 binding sites.

RESULTS

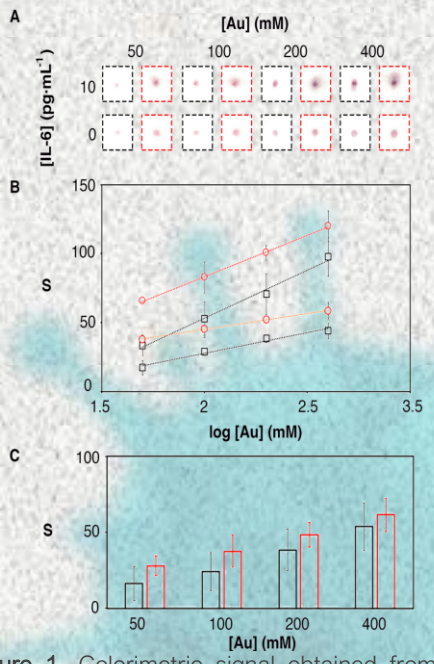

Figure 1. Colorimetric signal obtained from samples containing 0 or 10 pg·mL^{-1} when using 3 capture sites (CS) and the paper is folded so that the 3 signals add up (red) or unfolded and measuring only CS1 (black); (A) Photographs of the assays; (B) Colorimetric signal for 10 (dots) and 0 (squares) pg·mL^{-1}; (C) Specific signal after subcontracting 0 from 10 pg·mL^{-1}; Error bars are the standard deviation (n=3).

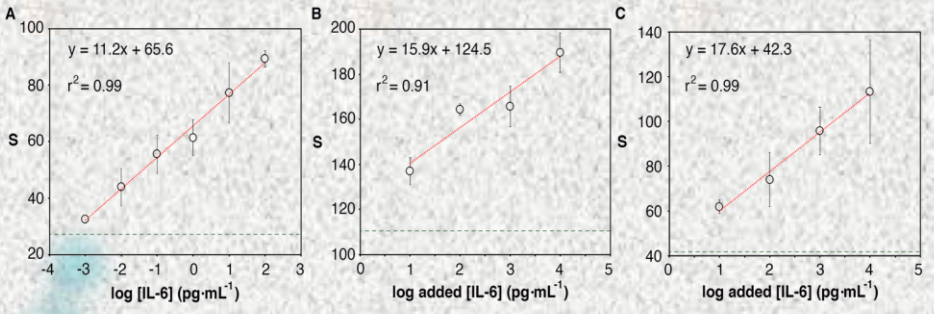

Figure 2. Detection of IL-6 in PBS (A), or spiked into blood (B), or bronchial aspirate (BAS, (C)). Horizontal dotted lines represent the signal above 3 times the standard deviation of the blank. Error bars are the standard deviation (n=3).

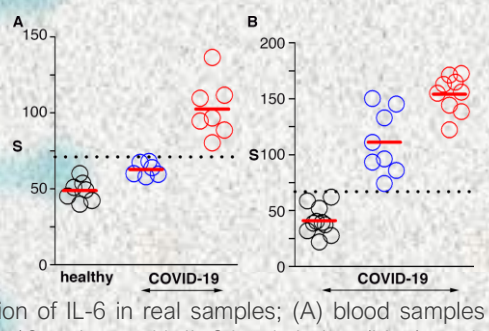

Figure 3. Detection of IL-6 in real samples; (A) blood samples from healthy donors (black) or COVID-19 patients with IL-6 levels below (blue) or above (red) 17 pg·mL^{-1}. (B) Bronchial aspirate (BAS) samples from COVID-19 patients with IL-6 levels below 10 pg mL^{-1} (black), between 10 and 100 pg mL^{-1} (blue), or above 100 pg mL^{-1} (red). Dotted lines show the average signal plus 2 times the standard deviation of healthy donors or patients with IL-6 below 3 pg·mL^{-1} (black).

CONCLUSION

In conclusion we have introduced paper immunosensors with a mobile readout platform for the detection of IL-6 in blood and respiratory samples from COVID-19 patients. The immunosensors have a low limit of detection at 10^{-3} pg mL^{-1} and a wide dynamic range over 5 orders of magnitude due to their paper-based signal generation design. Thanks to this procedure, we were able to correctly classify blood samples from COVID-19 patients with an IL-6 content higher than 17 pg mL^{-1}, and BAS samples above 10 pg mL^{-1}. The tests are lightweight, easy to transport and distribute, and easy to dispose of by incineration. Our app does not require any accessory to control photographic conditions, making it particularly useful for home testing. These features make the proposed biosensors a promising tool for the decentralized management of COVID-19 patients at home or in hospital.

REFERENCES

[1] Huang, C.; Wang, Y.; Li, X.; Ren, L.; Zhao, J.; Hu, Y.; Zhang, L.; Fan, G.; Xu, J.; Gu, X.; et al. Clinical Features of Patients Infected with 2019 Novel Coronavirus in Wuhan, China. *Lancet* **2020**, *395* (10223), 497–506. https://doi.org/10.1016/S0140-6736(20)30183-5.

[2] Hollander, J. E.; Carr, B. G. Virtually Perfect? Telemedicine for Covid-19. *N. Engl. J. Med.* **2020**, *382* (18), 1679–1681. https://doi.org/10.1056/NEJMp2003539.

[3] Russell, S. M.; Alba-Patiño, A.; Barón, E.; Borges, M.; Gonzalez-Freire, M.; De La Rica, R. Biosensors for Managing the COVID-19 Cytokine Storm: Challenges Ahead. *ACS Sensors* **2020**, *5* (6), 1506–1513. https://doi.org/10.1021/acssensors.0c00979.

Naked-Eye assessment of polymorphonuclear leukocytes activation status with plasmonic nanosensors

Giulia Santopolo, Antonio Clemente*, Alberto del Castillo, María Aranda, Antonia Socias, Marcio Borges and Roberto de la Rica*

Sepsis multidisciplinary Group

Introduction

Evaluating polymorphonuclear cells (PMNs) degranulation status is a key factor in determining the inflammatory response in case of severe infection or sepsis. For this reason assessment of PMNs activation by flow cytometry is a useful tool to monitoring the host response in septic patients. However, this technique requires complex and expensive instrumentation. Here, we propose a new biosensor based on the electrostatic interaction between granular basic proteins (such as myeloperoxidase [MPO], or elastase) and gold nanoparticles (AuNPs), giving a color shift (Fig.1) visible at naked-eye.

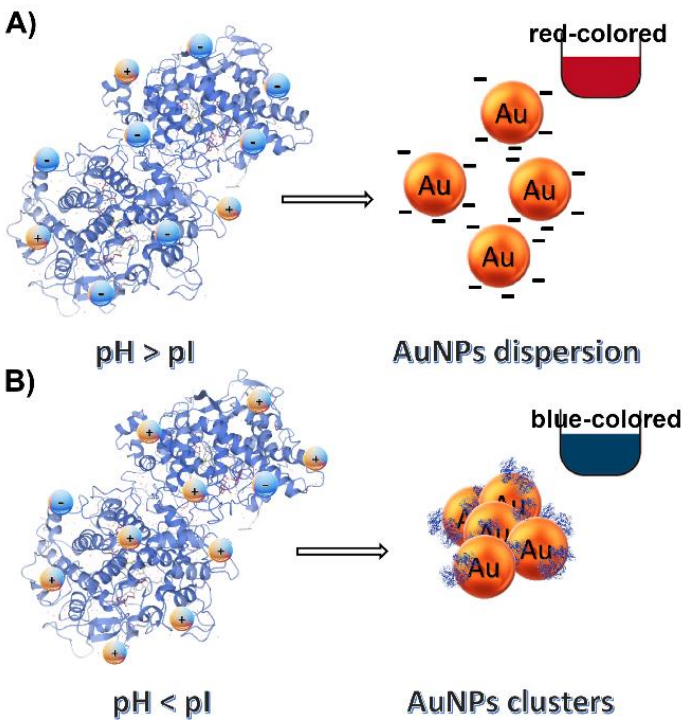

Fig. 1. Protein-guided AuNPs assembly. ***A)*** Negative surface-charged proteins in contact with AuNPs yield a red solution; ***B)*** Positive surface-charged proteins interact with AuNPs forming clusters and giving a blue-colored solution.

Methods

Cells purification and stimulation: total PMNs were purified from blood of healthy donors or patients using a EasySep™ Human Pan-Granulocyte isolation kit (Fig. 3A). Then, PMNs were cultured in RPMI and activated with 2.5 μM ionomycin during 15 min at 37 ºC. Activation of PMNs was confirmed after evaluation of CD63 expression by flow cytometry (Fig. 3B).

MPO as a proof-of-concepts: Purified MPO (pI 9.2) was mixed with AuNPs at different pH (phosphate buffer, 10mM) to observe the color pattern in ideal conditions (Fig.2); the same experiment was repeated with glucose oxidase (GOx; pI 4.2). AuNPs aggregated in the presence of MPO at very low concentration (Fig.2 A), while GOx did not affect the AuNPs stability (Fig.2 B).

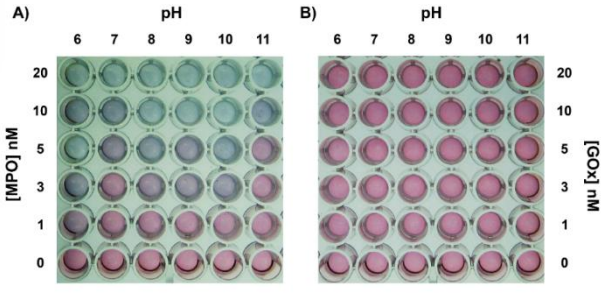

Fig. 2. Behaviour of AuNPs mixed with **A**) MPO or ***B)*** GOx at different pH [6;11]. Greater aggregation is drived by MPO while GOx does not give any color shift.

Results

Our biosensor was first tested in several healthy donors; AuNPs still aggregated with samples diluted up to 1:1000 only when supernatants (SNs) from activated PMNs cultures (enriched with granular basic proteins) were used (Fig. 5A) Next, the same test was tried with septic patients; as their PMNSs are already degranulated *in vivo* (Fig. 4), no further proteins will be released after ionomycin activation, resulting in a negative answer (Fig. 5B-C)

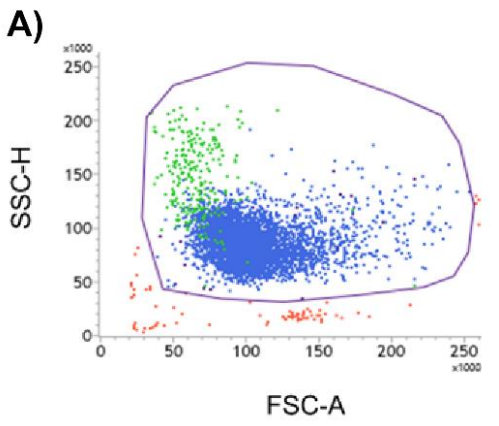

Fig. 3. Purification and stimulation of PMNs. **A)** SSC/FSC of purified PMNs; eosinophils (green) and neutrophils (blue). **B)** Degranulation evaluated by CD63 expression in unsitmulated (blue) and stimulated (orange) PMNs.

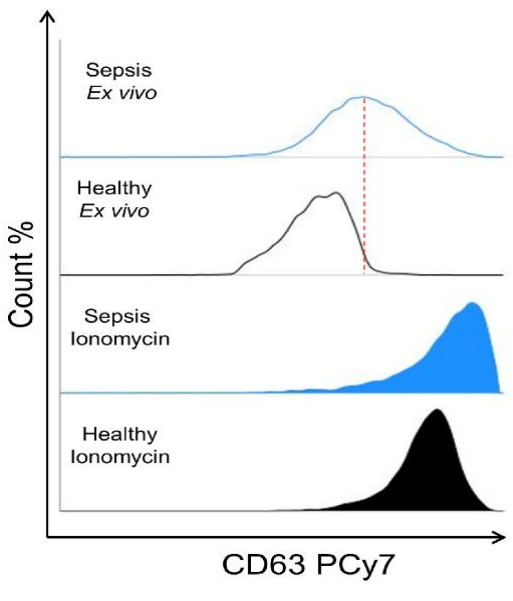

Fig. 4. CD63 expression in PMNs from a septic patient (blue) or a healthy control (black), *ex vivo* (open histograms) or after ionomycin activation (filled histograms). Basal levels of degranulation marker CD63 are increased in septic patients.

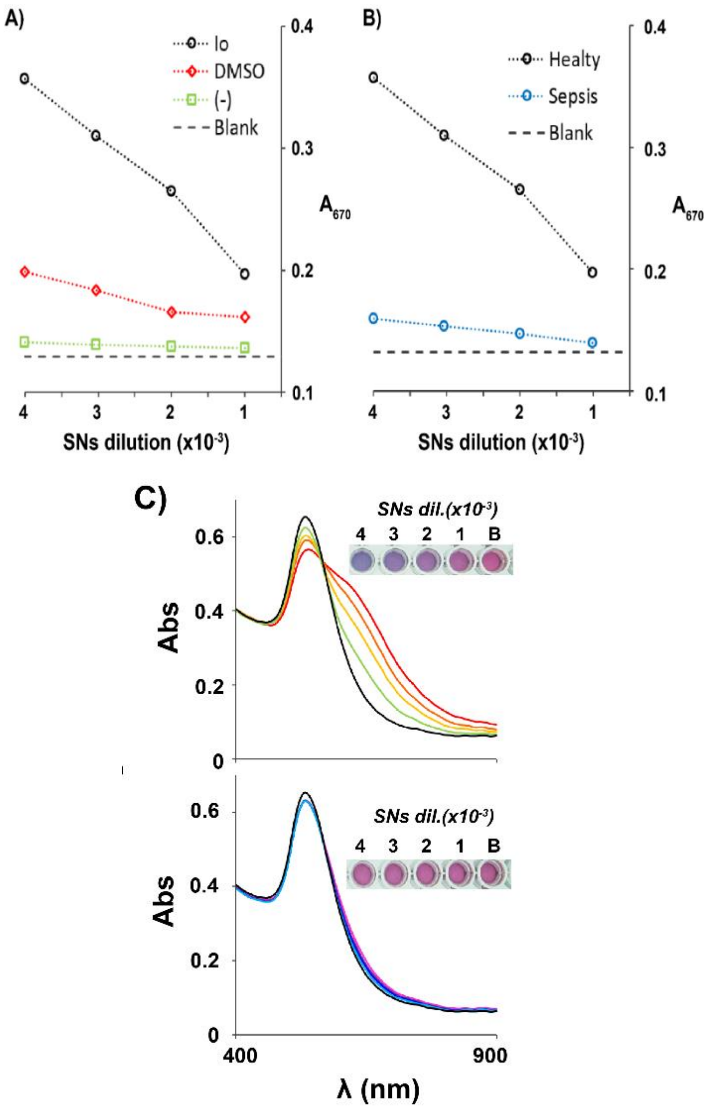

Fig 5. A) Absorbance values taken at 670nm for healthy donor (HD); SNs diluted in PB (10 mM, pH 6) with ionomycin (black), DMSO (red) or without any stimulation (green). ***B)*** Comparison between HD (black dots) and patient with sepsis (blue dots) both treated with ionomycin, by plotting absorbance at 670nm; ***C)*** Vis-NIR spectra representing diluted SNs samples from HD (top) and septic patients (bottom); color solution represented in the top rigth insert.

Conclusions

The biosensor based on cationic protein-guided AuNPs assembly is able to determine the PMNs degranulation status. Our test was tried on several healthy donors and septic patients, discerned by a different red-shift. Our device will be tested in a larger cohort of patients to improve its selectivity and reliability.

VII JORNADES IdISBa, Hospital Son Espases, 30/11-2/12, 2020

Impact of peptidoglycan recycling blockade and hyper-production of AmpC β-lactamases on *Enterobacter cloacae* virulence

Isabel María Barceló-Munar, Marina Ramírez-Cortés, Maria Escobar-Salom, Gabriel Torrens, Elena Jordana-Lluch, Carlos Juan* & Antonio Oliver.
Servicio de Microbiología, Hospital Universitari Son Espases-Fundación Instituto de Investigación Sanitaria de Baleares (IdISBa), Palma, Spain.
www.arpbigidisba.com

Introduction & Objectives

Enterobacter cloacae (EC) is one of the most important nosocomial gram-negative pathogens, in fact belonging to the ESKAPE group, whose clinical importance relies on their virulence and great capacity for antibiotic resistance development and dissemination. In the current scenario of effective antibiotics' shortage, to understand the interplay between antibiotic resistance and pathogenesis is essential to obtain clues for the development of therapies intended to attenuate EC virulence. Previously, we showed that the simultaneous combination of: i) peptidoglycan (PGN) recycling blockade, and ii) hyper-production of the chromosomal AmpC β-lactamase causes a dramatic impairment in the fitness and virulence of *Pseudomonas aeruginosa* (PA), which is another of the main opportunistic gram-negative pathogens (Pérez-Gallego M. *et al*, MBio, 2016). Through the present work we sought to check if these observations could be applicable to EC, or if certain specific particularities may exist in this context.

Materials & Methods

Bacterial strains and plasmids: EC subsp. *cloacae* strain ATCC 13047 was used as wildtype. An *ampG-defective* mutant was constructed following previously published protocols (Huang T. *et al*, BMC Protocols, 2014). An spontaneous AmpC hyperproducer mutant (ca. 120-fold compared to wildtype *ampC* expression, checked by RT-PCR) was obtained through culturing with cefotaxime 4 mg/L, and whose molecular basis was a frameshift mutation in *ampD* (Fig. 1), as proved by DNA sequencing. The multicopy plasmid pUCPACpa, containing the cloned PA PAO1 strain's *ampC*, was transformed into the wildtype and *ampG-defective* EC strains, providing an AmpC hyperproducer phenotype as well (as proved by β–lactam susceptibility profiles). The cloning vector pUCP24 was also transformed into this latter strain, which was used as a control.

Invertebrate infection model: To assess virulence, the infection through injection in *Galleria mellonella* larvae (Trularv, Biosystems Technology) was performed with different bacterial dosages ($5E^5$-$5E^7$ CFU in a final volume of 10 µL/larva), monitoring mortality at 24, 48, 72 and 96h at 30ºC. The survival data from 3 independent experiments were plotted using the Kaplan-Meier method and differences were analyzed using the log-rank test, considering a P value < 0.05 as statistically significant in the pairwise comparisons.

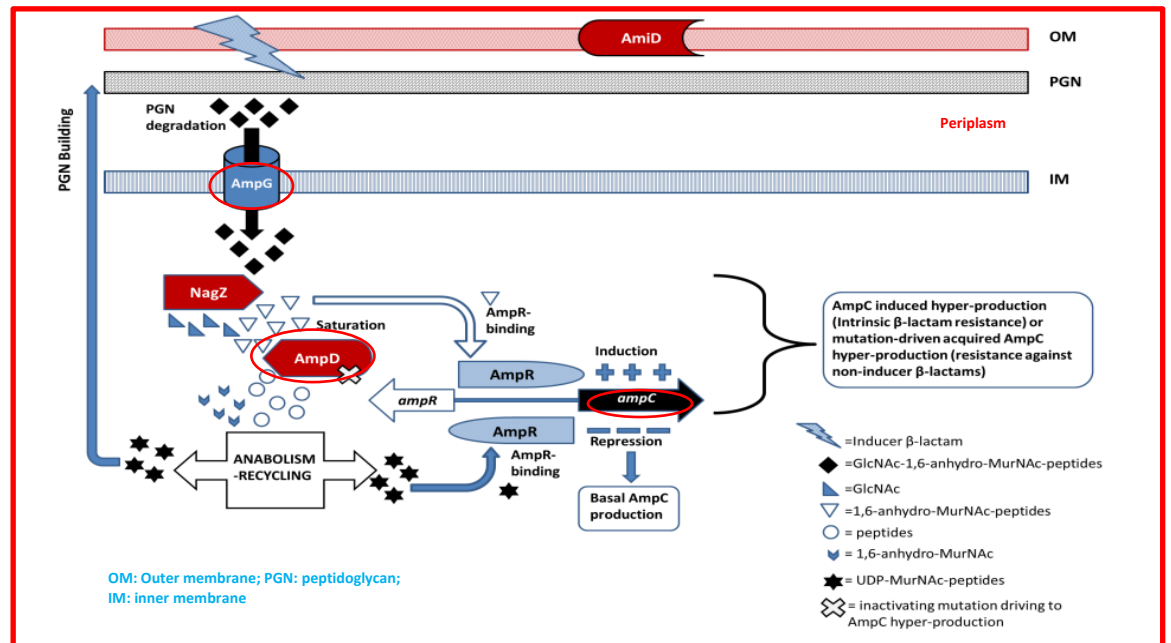

Fig. 1. *E. cloacae* AmpC regulatory pathway and PGN recycling: two closely related processes. AmpG (acting as cytosolic gate for the released PGN fragments) whose deletion drives to recycling blockade, and AmpD (an indirect repressor of AmpC β–lactamase, that also takes part in PGN recycling), are displayed within red circles as main characters of this work.

Results

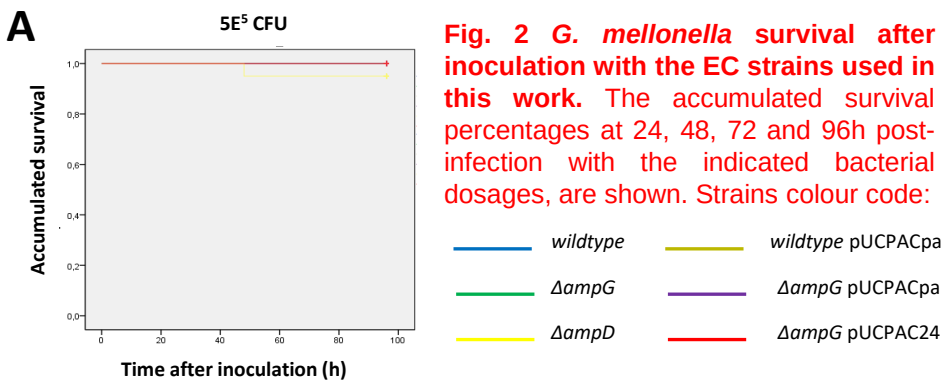

Fig. 2 *G. mellonella* survival after inoculation with the EC strains used in this work. The accumulated survival percentages at 24, 48, 72 and 96h post-infection with the indicated bacterial dosages, are shown. Strains colour code: *wildtype*, *wildtype* pUCPACpa, Δ*ampG*, Δ*ampG* pUCPACpa, Δ*ampD*, Δ*ampG* pUCPAC24.

As can be observed in the Figure 2A/B, at the two lowest bacterial doses no differences among strains were appreciable. Moreover, the inactivation of *ampG* apparently did not have a significant impact over virulence at any bacterial dose (P > 0.05 compared to wildtype). Conversely, the AmpC hyper-production *per se* significantly attenuated EC virulence. To cite just one example, for the $1.25E^7$ CFU dosage (Fig 1C) the survival rates at 96h for wildtype and Δ*ampG* strains were ca. 20-30%, whereas for the strains wildtype pUCPACpa, Δ*ampG* pUCPACpa and Δ*ampD* the survival was always above 50%, with respective P values of 0.002, <0.0001 and 0.024, in the comparison with Δ*ampG* strain. These results suggested a greater impact of PA AmpC over EC virulence, than that caused by the intrinsic EC enzyme hyper-production. This trend was also confirmed at the highest dose (Fig 2E), with P values of <0.0001, 0.001 and 0.009 respectively. No statistically significant differences among wildtype, Δ*ampG* and Δ*ampG* pUCP24 strains were found in any case.

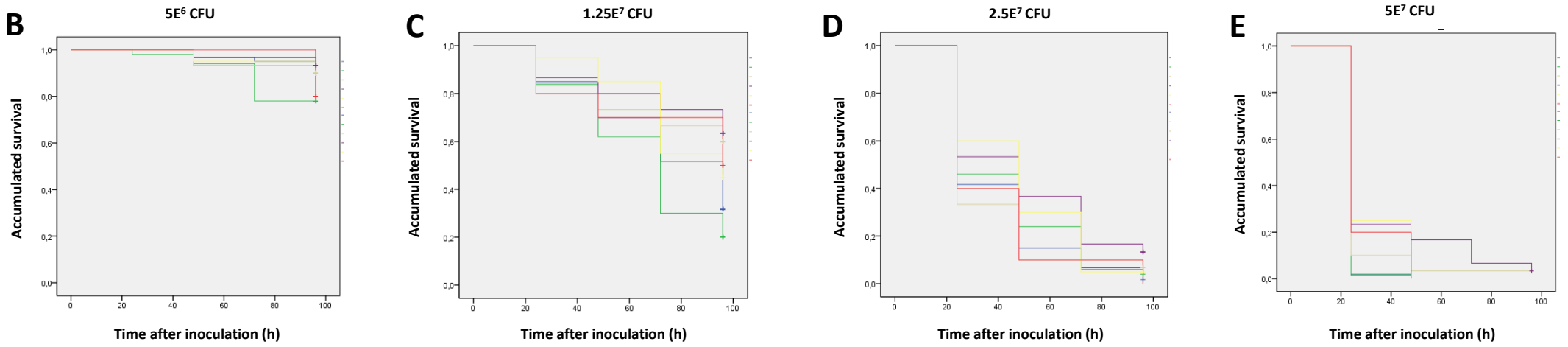

Conclusions

The hyperproduction of the intrinsic AmpC β-lactamase (or of the PA enzyme) *per se* entails a notable attenuation of EC virulence. A potential residual activity of AmpC (apparently even stronger in the case of the PA enzyme) over the EC cell-wall, driving to its degradation and consequent loss of viability and virulence, could explain the obtained results, to which the PGN recycling impairment may also contribute. Here we show some differences and similarities between the resistance/cell-wall biology/virulence interplay in PA vs EC, suggesting the existence of weak points useful for the design of future anti-virulence therapeutic strategies.

ACKNOWLEDGEMENTS: This work was supported by the Spanish Network for the Research in Infectious Diseases (RD16/0016) and grants PI18/00681 and PI18/00076, Instituto de Salud Carlos III, cofinanced by the European Regional Development Fund. We especially thank **Aina Rosa Millán** from the IdISBa CLINICAL TRIALS & METHODOLOGY SUPPORT PLATFORM, for her assistance in the statistical analysis and graphic representation of the data.

Sistema d'Informació Geogràfica anonimitzat per donar suport a la lluita contra la pandèmia COVID-19.

Josep Muncunill Farreny[1], Joan Albert Pou Goyanes[1,2], Maurici Ruiz Pérez[3], Antoni Colom Fernández [1]
1 Institut de Investigació Sanitària Illes Balears (IDISBA), 2 Hospial Unibersitari Son Espases, 3 Universitat de les Illes Balears (UIB), Spain

Introducció i Objectius

- La informació sanitària és altament sensible donada la seva confidencialitat i requereix ser anonimitzada per a realitzar estudis d'investigació.
- La geolocalització dels casos infectats per SARS-CoV-2 es un exemple de la sensibilitat de la informació i alhora de la seva utilitat per estudiar l'evolució de la malaltia.
- La aplicació desevolupada permet anonimitzar la informació sanitària geocodificada i subministrar dades a centres d'investigació per donar suport a la gestió de la pandèmia.

Mètodes

L'aplicació s'ha desenvolupat en R Shiny. Permtet anonimitzar la informació dipositada assignant un ID a cada individu i treballar les dades impedint la identificació de l'individu.
La agregació de les dades es fa diferents nivells geogràfics (Comunitat Autònoma, Municipi, Cens), i permet la seva correlació amb altres variables georeferenciades com els recursos socioeconòmics dels barris.

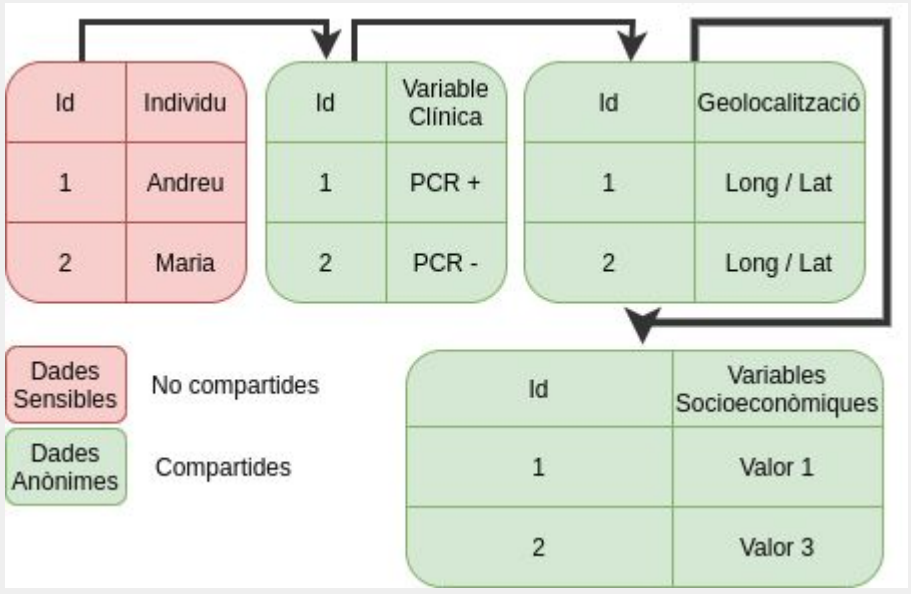

Fig.1 Esquema de creuament d'informació

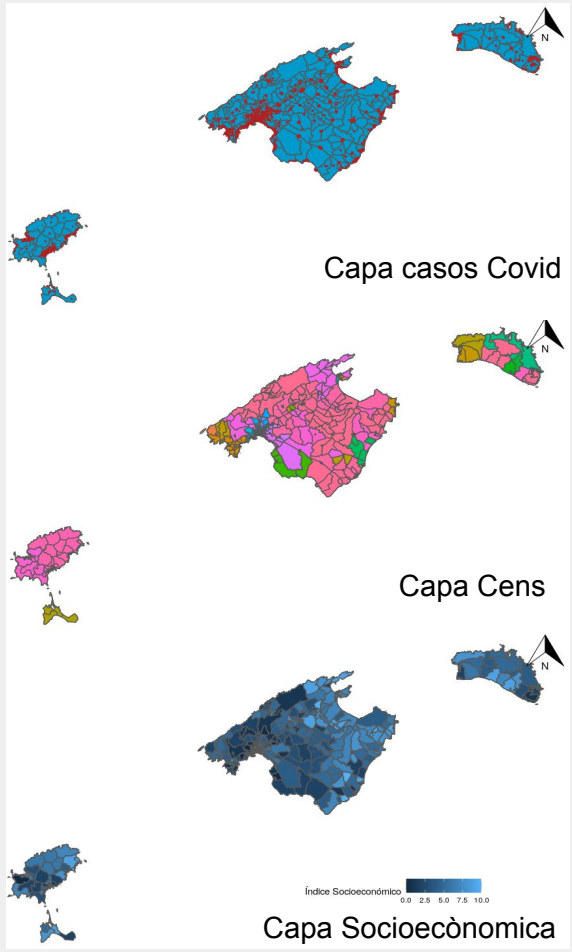

Fig.2 Capes amb informació georeferenciada

Resultats

Mapes de calor

Mapes d'incidència acumulada

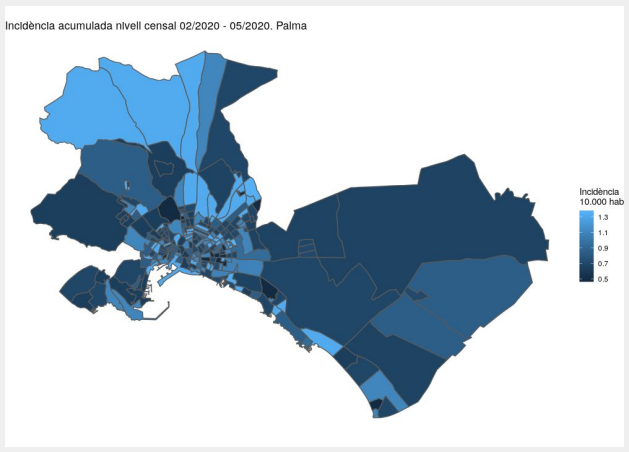

Correlació variables clíniques i socioeconòmiques

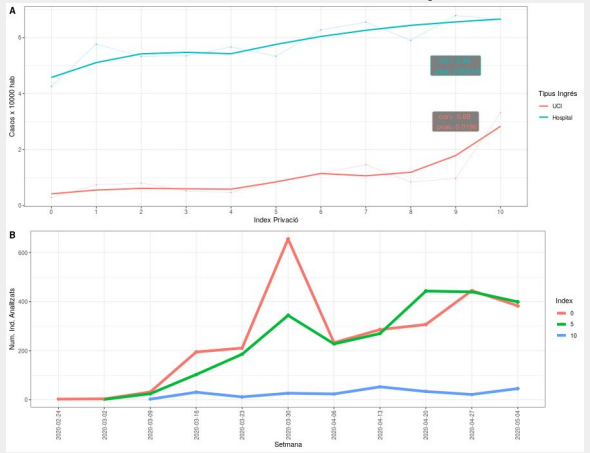

Fig. 3 Diferents visualitzacions dels anàlisis amb la informació del COVID

Discussió

La anonimització és un pas clau per garantir la investigació amb dades sensibles.
La aplicació desenvolupada es garanteix la assignació d'un ID a la informació confidencial, de manera que sigui impossible recuperar la identitat dels individus i permet la usabilitat de les dades per a la recerca i presa de decisions.
L'aplicació s'ha servit per a fer els anàlisis de les dades del projecte SIG-COVID-19, a on s'analitza el possible impacte que tenen els recursos socioeconòmics a nivell censal a les Illes Balears en la evolució del SARS-CoV-2.

Time-course of β-lactam antibiotics target-site penetration and binding to penicillin-binding proteins (PBP) in isolated membranes and intact cells of *P. aeruginosa*

María Montaner, Silvia López and Bartolomé Moya

Servicio de Microbiología and Unidad de Investigación, Hospital Universitario Son Espases, Instituto de Investigación Sanitaria Illes Balears (IdISBa), Palma de Mallorca, Spain

Introduction:

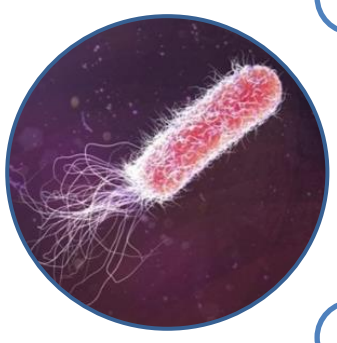

- *Pseudomonas aeruginosa* is one of the major nosocomial gram-negative pathogens. Serious global health threat
- Outer membrane (OM) represents the limiting barrier for the target site penetration of many antibiotic
- High ability for antibiotic resistance development (β-lactamase, porins, efflux pumps)
- Efficacious antimicrobial options are severely limited
- Measuring the OM-permeability and PBP binding of β-lactams is fundamental to develop optimized therapies

Objetive:

Study the time-course of target-site penetration and binding of 11 chemically different β-lactams and 4 β-lactamase inhibitors (BLI) in isolated membranes and intact cells of *P. aeruginosa* PAO1.

Material and methods:

To assess the binding rates and permeability of *P. aeruginosa*, two different methodologies were used.

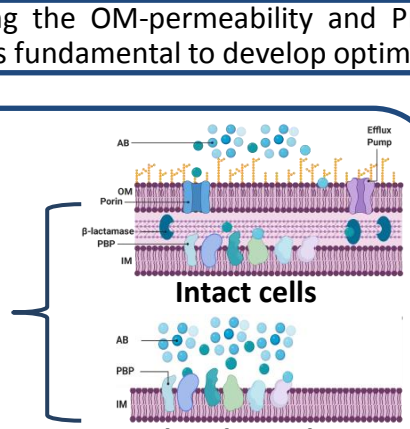

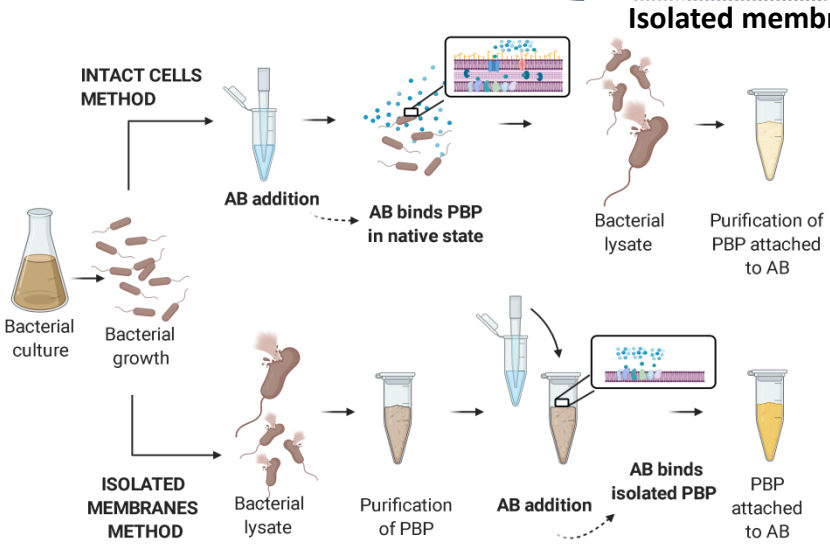

PBP-binding affinities at 15, 30 and 60 minutes in isolated membranes and intact cells were determined by Bocillin FL assay using 2 × MIC of each compound (BLI were used at 4 µg/mL fixed concentration).

Time-course PBP occupancy assay showed:

- The highest rate of penetration for **carbapenems** (except ertapenem). Highest affinity was observed for PBP2, 4 and 5/6, displaying minor differences in PBP occupancy between intact and lysate cells.
- **Cephalosporins**, especially cefepime, displayed a much slower binding (preferentially to PBP1a and 3).
- **Aztreonam** showed remarkable differences in PBP binding rate and profile.
- **Penicillins** displayed much slower PBP occupancies (PBP1a, 1b, 3) for the intact cells assay.

Results:

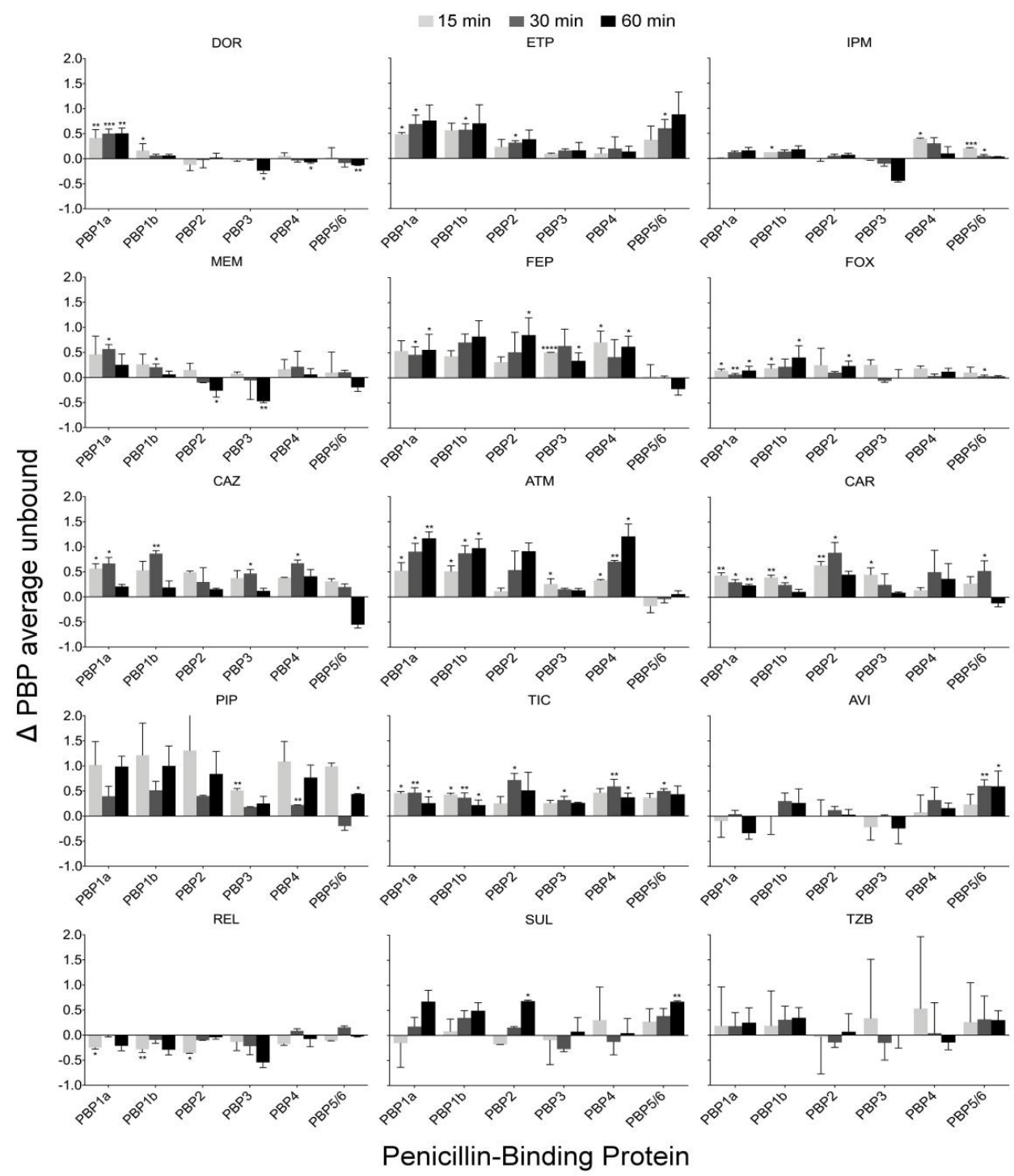

- **BLI**, particularly tazobactam and relebactam, showed a barely discernible binding both in lysed and intact cells, whereas avibactam and sulbactam displayed modest PBP binding in the lysate cells assay, mostly for PBP2, 4 and 5/6.

Conclusions:

- We created the **first intact cells PBP binding dataset** for chemically diverse β-lactams and β-lactamase inhibitors in ***P. aeruginosa***.
- **Carbapenems** were the class showing **faster rate** of binding kinetics and among them, **Imipenem** was the **fastest**.
- We found **differences not only** in the **binding rate but also in the affinity profile** of the PBP in intact cells and isolated membranes.
- In order to **optimize therapies** against **MDR *P. aeruginosa***, it is i**mportant to measure PBP binding in intact cells**, since it allows us to categorize antibiotics not only by their **binding affinity** to their targets but also by their **ability to penetrate** through the outer membrane as well as their efflux and β-lactamase hydrolysis.

What clinical variables are associated with a worse prognosis in patients with COVID-19 ?. Comparison with severity scales CURB and News2

M.I. Fullana [1], H.H. Vilchez [1], F. Alberti [1], A. Cañabate [1], F. Artigues [1], L. Planas [1], F. Figueras [1], M.A. Ribas [1], J. Murillas [1], F.J. Fanjul [1], M. Riera [1].

Grup de Malalties Infeccioses-VIH.Idisba. Hospital Universitario Son Espases - Palma (Spain)

Introduction and purpose

In the new COVID-19 infection, it is very important to know the clinical variables, which can be obtained at the patient's home associated with a poor prognosis. It is also important to know which severity scales may be more useful for emergency services or general practitioner to decide wich patients need referral to the hospital.

Methods

All the patients admitted to the HUSE by COVID -19, with a diagnosis confirmed by PCR, from February 15 to May 15, 2020 were included. A standardized clinical data collection form was used prospectively. Only clinical-epidemiological and anamnesis data on admission were used. The evolution to death, admission to the ICU or need for invasive mechanical ventilation (IMV) was considered an adverse outcome. A univariate and multivariate analysis of the variables related to adverse outcome was performed. The model obtained was compared with the CURB and NEWS2 severity scales.

Results

362 patients were included, with a mean follow-up of 22.6 days (SD 9.5). 50 required ICU admission (13.8%), IMV 36 (10.2%) and NIMV 14 (4%), 54 (14.9%) died, and overall, 89 patient (24.6%) had an adverse outcome. Other complications observed were: bacterial pneumonia 26 (7.3%), ARDS 89 (24.9%), ECVA 3, PET 15 (4.3%), Heart failure 13 (3.6%), arrhythmias 12 (3 , 3%), bacteremia 17 (4.7%), FRA 52 (14.7%), liver failure 9 (2.5%), HDA 6 (1.7%).

The variables related to adverse outcome in the univariate analysis (table 1) were: Being male OR 3.44 (2-6.25), being > 60 years OR 2.59 (1.54-4.3), presenting comorbidities mainly HTA OR 1.7 (1.05-2.7), CKD OR 2.3 (1.09-4.9), diabetes mellitus OR 1.94 (1.1-3.4). Present as symptoms dyspnea OR 3.72 (2.13-6.48) or confusional state OR 2.52 (1.22-5.16), or have tacypnea on examination FR> 24 x 'OR 3.93 (2 , 3-6.8), or tachycardia FC> 90 OR 1.72 (1.06-2.79) or SO2 <90% OR 10.8 (5.4-21.6).

In the multivariate analysis, if we did not enter SO2, only age OR 2.6 (1.19-5.7), being male OR 3.2 (1.68-6.1>), presenting dyspnea OR 2.8 (1.49-5.5) and tachypnea FR> 24 x 'OR 2.42 (1.26-4.64), the AUC with this model was 0.78 (0.72-0 , 84). If we consider SO2 in the model, male OR OR 2.56 (1.28-5.1), dyspnea OR 2.32 (1.15-4.56) and SO2 <90% OR 1 were included in the model. 22 (1.12-1.31). With this model, the AUC to predict an adverse outcome was 0.82 (95% CI 0.77-0.88) fig 1. If we compare with the severity scales the AUC of the CURB scale was 0.75 (0.68-0.82) and with the NEwS2 scale 0.87 (0.81-0.93) fig 2.

Results

Table 1: Variables associated with a poor COVID prognosis .

Variables	Good outcome N:273	Poor outcome N:89	p signif	OR (CI 95%)
Sexe (male) N(%)	136 (49,8)	69 (77,5)	<0,0001	3,44(2-6,5)
Age>60 y N(%)	135 (49,4)	64 (71,9)	<0,0001	2,59(1,54-4,3)
HTA N(%)	110 (40,2)	47 (52,8)	0,03	1,781,05-2,7)
CKD N(%)	19 (6,9)	13 (14,6)	0,025	2,3(1,09-4,99
COPD N(%)	11 (4)	12 (13,4)	0,004	
Diabetes mellitus N(%)	44 (16,1)	24 (26,9)	0,021	1,94(1,1-3,4)
Two or more comorbidities N(%)	112 (41)	49 (55)	0,017	1,8 (1,1-2,9)
Dysnea N(%)	126 (46,1)	67 (75,3)	<0,00001	3,72(2,13-6,48)
Confusion N(%)	20 (7,3)	15 (16,8)	0,01	2,5(1,2-5,1)
HR <90 x' N(%)	119 (43,5)	51 (57,3)	0,026	1,72(1,06-2,8)
BR>24 x N(%)	71 (26)	49 (55)	<0,0001	3,93(2,3-6,8)
CURB >=2 N(%)	72 (26,3)	49 (55)	<0,0001	6,36(3,3-12,3)
NEWS-2 >4 N(%)	61 (22,3)	46 (51,7)	<0,0001	16,2(6,5-40)
SO2 %	95	89	<0,0001	

Figure 1. Multivariate model obtained AUC

AUC. Multivariant model

Área	Desv. Error[a]	Significación asintótica[b]	95% de intervalo de confianza asintótico Límite inferior	Límite superior
,824	,029	,000	,768	,881

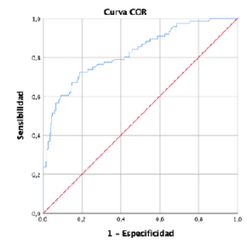

Figure 2. NEWS2 scale AUC

Variables de resultado de prueba: ES_NEWS2

Área	Desv. Error[a]	Significación asintótica[b]	95% de intervalo de confianza asintótico Límite inferior	Límite superior
,873	,028	,000	,817	,929

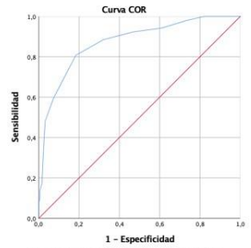

Los segmentos de diagonal se generan mediante empates.

Conclusions

Approximately 25% of the patients admitted presented complications, 14% required ICU admission. In the multivariate analysis, being male, being> 60 years old, presenting dyspnea and tachypnea on admission were associated with a poor prognosis. If we included SO2 in the multivariate model, being male, presenting dyspnea and having SO2 <90% were the only variables included. Either of these 2 models was lower than the NEWS2 severity scale to predict poor evolution

ESTANDARDITZACIÓ D'UN PROTOCOL PER LA DETECCIÓ D'ESPÈCIES REACTIVES D'OXIGEN (ROS) PER CITOMETRIA DE FLUX

M. Berman; V. Cunill; L. Mañogil; A. López-Gómez; A. Clemente; V. Andreu; MA. Estévez; J. Pons; JM. Ferrer.

Grup Estudi de la Resposta Immunològica en Patologia Humana, Institut d'Investigació Sanitària de les Illes Balears (IdISBa)

INTRODUCCIÓ

- Les especies reactives d'oxigen (ROS) són molècules de curta vida altament reactives que es produeixen a partir de superòxid o reduccions incomplertes i que poden interactuar amb diverses molècules intracel·lulars (àcids nucleics, lípids, proteïnes, etc.).
- La correcta regulació de les ROS és fonamental per la supervivència, creixement, proliferació i diferenciació cel·lular[1]. Tradicionalment han estat considerades molècules "tòxiques" per a les cèl·lules i teixits i s´han relacionat amb diferents patologies humanes com la inflamació crònica o les malalties relacionades amb l'edat i el càncer.
- Investigacions recents posen de manifest el paper d'aquestes substàncies en la funcionalitat de les cèl·lules del sistema immunitari[2]. És important identificar les fonts de ROS, el seu paper en els processos de senyalització i les seves conseqüències funcionals en els diferents tipus cel·lulars.

OBJECTIU

Estandardització d'un protocol ràpid i senzill per la detecció de ROS en diferents subpoblacions limfocitàries per citometria de flux.

METODOLOGIA

- Cèl·lules mononucleades de sang perifèrica (PBMC) es cultiven en presència o absència d'inductors de producció de ROS (Tert-butyl hydroperoxide; TBHP), antioxidants (N-acetylcysteine; NAC) i estímuls específics per l'activació de les diferents subpoblacions limfocitàries. S'estudia l'expressió cel·lular de ROS (CellRox Deep Red Reagent), la viabilitat cel·lular (SYTOX Blue Cell Dead Stain) i s'identifiquen cèl·lules amb marcadors específics per cada subpoblació (anti-CD3 (Limfòcits T); anti-CD19 (Limfòcits B); anti-CD27 (L. B de memòria), etc.). Les mostres s'analitzen per citometria de flux ajustant la compensació i s'avaluen els resultats.

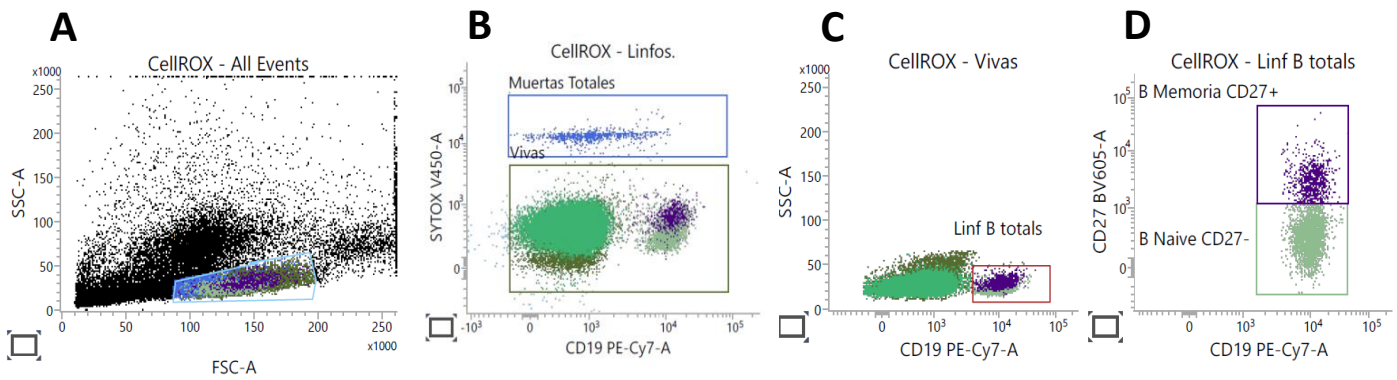

Figura 1. Estratègia de gateig per citometria de flux de les cèl·lules limfocitàries d'interès mitjançant l'expressió de diferents marcadors: (B) cèl·lules vives (SYTOX-); (C) Limfòcits B totals (CD19+); (D) Limfòcits B de memòria (CD27+CD19+) i limfòcits B naive (CD27-CD19+).

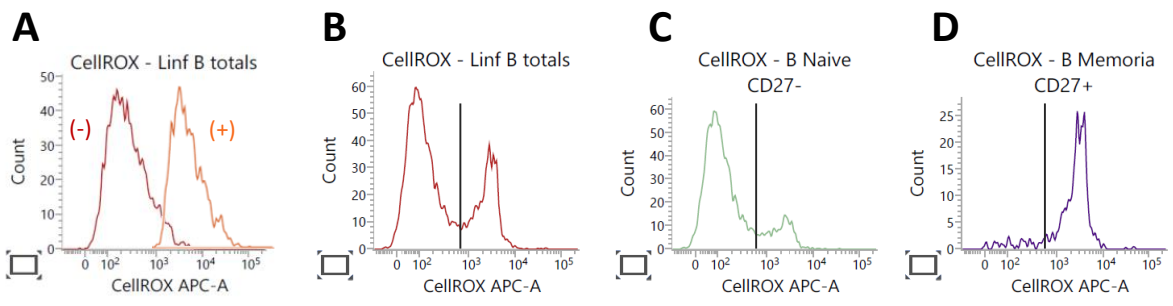

Figura 2. Expressió de ROS en diferents poblacions cel·lulars. **A)** Control positiu i negatiu. (+) Mostra incubada amb l'inductor de ROS (TBHP); (-) Mostra incubada amb l'inductor de ROS (TBHP) i amb antioxidant (NAC) per verificar la disminució de ROS. **(B-D)** Expressió basal de ROS en diferents subpoblacions limfocitàries: **(B)** Limfòcits B totals (CD19+), **(C)** B naive (CD27-CD19+) i **(D)** B memòria (CD27+CD19+).

RESULTATS

- S'han avaluat les concentracions i temps d'incubació òptims per cada reactiu, aconseguint l'estandardització de la tècnica amb un temps total inferior a **3 hores.**
- La tècnica permet avaluar l'increment en la producció de ROS després d'**estimulació** amb l'inductor d'oxidació (control positiu); aquesta inducció s'anul·la en presència d'**antioxidant** (control negatiu) (Fig. 2 A).
- Diferents subpoblacions limfocitàries produeixen de forma basal **diferents nivells de ROS** (Fig. 2 B, C i D) i aquests es modulen després de l'activació amb estímuls específics.

CONCLUSIONS

L'estandardització d'aquest mètode relativament **senzill** i **ràpid**, ens permet l'estudi de les ROS en les diferents subpoblacions del sistema immunitari en mostres de sang perifèrica. Pel laboratori d'Immunologia, aquest protocol suposa un **gran avenç** ja que permetrà investigar el paper de les ROS en diferents patologies com les immunodeficiències primàries.

1. Yuhui Yang, Alexandr V. Bazhin, Jens Werner & Svetlana Karakhanova (2013) Reactive Oxygen Species in the Immune System, *International Reviews of Immunology*, 32:3, 249-270
2. Zhang H, Wang L, Chu Y. Reactive oxygen species: The signal regulator of B cell. *Free Radic Biol Med*. 2019 Oct;142:16-22.

La cirugía citorreductora (CRS) y la quimioterapia intraperitoneal hipertérmica (HIPEC) inducen un incremento de las poblaciones Th17 y T reguladora en pacientes con carcinomatosis peritoneal de origen colorrectal y ovárico

Miguel A. Estévez [1,4], Carla Soldevila [3,4], Neus Esteve [2,4], Juan J. Segura [3,4], Ana M. Ferrer [2,4], Valero Andreu[1,4], María Berman [1,4], Rafael Morales [3,4], Jaime Pons [1,4].

Departmentos de Inmunología [1],Anestesia[2] y Cirugía[3]. Hospital Universitari Son Espases. Institut d'Investigació de les Illes Balears (IdISBa)[4].

INTRODUCCIÓN Y OBJETIVOS

La diseminación peritoneal es la principal ruta de metástasis en pacientes con cáncer de ovario (CO) y unas de las principales en cáncer colorrectal (CC). El uso de la cirugía citorreductora (CRS) seguido de la quimioterapia hipertérmica intraperitoneal (HIPEC) ha permitido ampliar la esperanza de vida de estos pacientes y supone una alternativa terapéutica, potencialmente curativa, para la carcinomatosis peritoneal.

El sistema inmunológico juega un importante papel en el control y eliminación de las células tumorales. Los linfocitos T helper son los coordinadores de esa respuesta, encargándose de reclutar a las poblaciones de células efectoras necesarias. Las distintas subpoblaciones de linfocitos T helper (Th1, Th2, Th17 y Th17.1) generan diferentes patrones de citoquinas, dirigiendo así la respuesta celular y humoral del sistema inmunitario hacia el perfil más adecuado en función al tipo de agresión recibida por el organismo. Los linfocitos T reguladores (Treg) se encargan de inhibir la respuesta inmunitaria inicial, evitando así el posible daño derivado de su sobreactivación.

En el contexto del cáncer, la población Th1 es la principal promotora de la respuesta antitumoral. Por el contrario, la capacidad inhibitoria de los linfocitos T reguladores favorece la progresión de la enfermedad por falta de una respuesta inmunológica adecuada[1]. La población Th17 parece tener un papel dual, con una actividad protumoral asociada a la secreción de citocinas proinflamatorias, así como una actividad antitumoral debido al reclutamiento de otras poblaciones capaces de combatir el tumor[2].

Nuestro objetivo es caracterizar la distribución de las subpoblaciones de linfocitos T helper y Treg, en situación basal y a las 24 horas de la CRS e HIPEC, en sangre periférica de pacientes con carcinomatosis peritoneal derivada de cánceres colorrectales u ováricos.

MATERIAL Y MÉTODOS

Analizamos la distribución de linfocitos T helper y Treg en sangre periférica de 36 pacientes intervenidos en el servicio de cirugía del Hospital Universitario Son Espases, diagnosticados de carcinomatosis peritoneal derivada de CC (n=17) o CO (n=19) y tratados con CRS e HIPEC. Las muestras de sangre periférica fueron obtenidas antes y 24 horas después de la CRS-HIPEC y analizadas mediante citometría de flujo empleando combinaciones de los siguientes anticuerpos monoclonales marcados con fluorocromos: anti-CD4-PCy5, anti-CD45RA-ECD, anti-CD127-FITC, anti-CD25-PCy5, anti-CD4-Pcy7 (Beckman Coulter) y anti-CXCR3-FITC, anti-CCR6-PCy7 (Biolegend). Las imágenes fueron analizados mediante el programa Kaluza (Beckman Coulter) y el análisis estadístico se realizó empleando Graph Pad Prism 5 software (San Diego, CA, USA).

RESULTADOS

Observamos un aumento de las poblaciones Th17 y Treg a las 24 horas de la CRS-HIPEC en pacientes con CC (p=0.007 y p=0.0003 respectivamente) y CO (p=0.0002 y p=0.045 respectivamente) al comparar las poblaciones antes y 24 horas después de la CRS-HIPEC (**Figs. 1 y 2**). Asimismo, observamos un descenso en la población Th1 únicamente significativo en el grupo de pacientes con CO (p=0.0002) (**Fig. 3**). No se encontraron diferencias significativas en el resto de poblaciones analizadas.

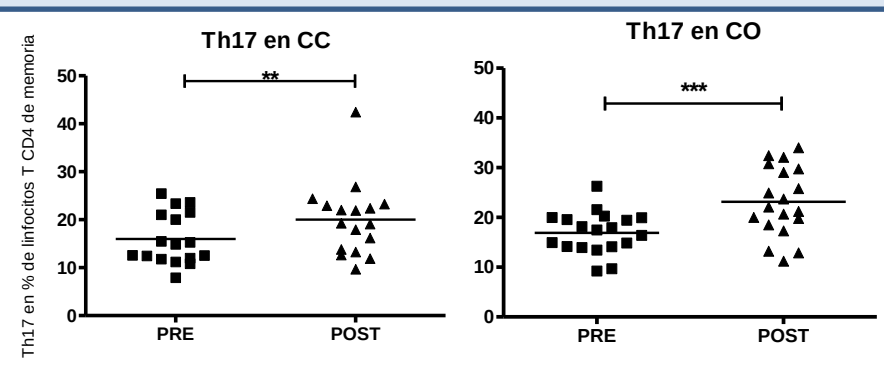

Fig. 1. Porcentaje de linfocitos Th17 del total de linfocitos T CD4+ de memoria antes y 24 horas tras la CRS-HIPEC en pacientes con cáncer colorrectal u ovárico.

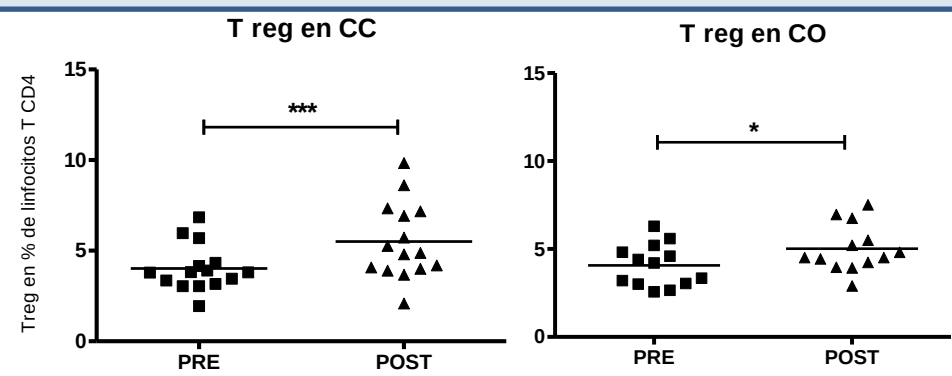

Fig. 2. Porcentaje de linfocitos Treg del total de linfocitos T CD4+ de memoria antes y 24 horas tras la CRS-HIPEC en pacientes con cáncer colorrectal u ovárico.

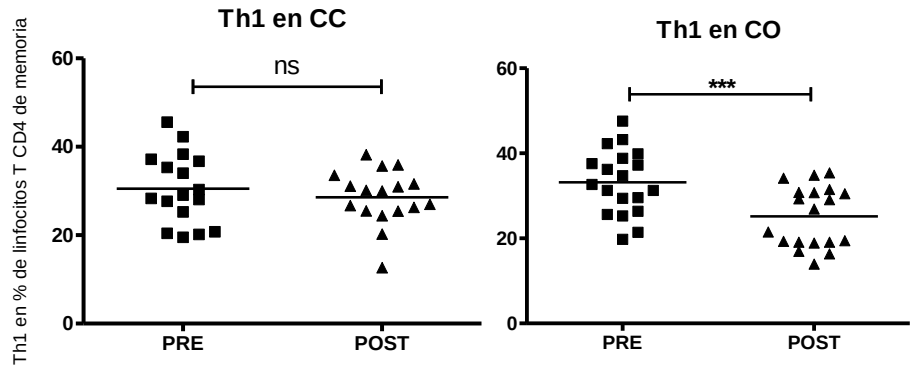

Fig. 3. Porcentaje de linfocitos Th1 del total de linfocitos T CD4+ de memoria antes y 24 horas tras la CRS-HIPEC en pacientes con cáncer colorrectal u ovárico.

CONCLUSIONES

La CRS e HIPEC inducen un incremento de las poblaciones de linfocitos Th17 y Treg en pacientes con cáncer colorrectal y ovárico, así como un descenso en la población Th1 sólo en pacientes con cáncer de ovario, factores que podrían favorecer el crecimiento tumoral. Ahondar en el conocimiento del papel que juegan las poblaciones linfocitarias Th17 y Treg en pacientes con carcinomatosis peritoneal podría posibilitar el uso de fármacos biológicos como terapia adyuvante y favorecer la respuesta anti-tumoral.

1. Chraa D, Naim A, Olive D, Badou A. T lymphocyte subsets in cancer immunity: Friends or foes. J Leukoc Biol. 2019 Feb;105(2):243-255
2. Punt S. *et al.* The correlations between IL-17 vs. Th17 cells and cancer patient survival: a systematic review. Oncoimmunology 2015 Mar 6;4(2)